Original Research Article

Linear Stability Analysis of a Delay Differential Integral Equation Motivated by Genetic Networks

Abstract

This work presents a computational study on the linear stability analysis of a genetic network with time delay. The network is modeled as a continuous system and takes the form of a nonlinear delay differential integral equation coupled to an ordinary differential equation. Analysis of the stable equilibria shows the existence of a critical time delay beyond which limit cycle oscillations are born in a Hopf bifurcation. We confirm our results by discretizing the continuous model into an N-dimensional system and showing that the associated critical time delays for the discrete system approach the critical time delay for the continuous system as N becomes large.

1 Introduction

Cells are formed of thousands of proteins and genes interacting in harmony to carry out the basic functions of life [1]. Understanding this network of interactions is an important part of biology and, more recently, applied mathematics. From a theoretical viewpoint, the network represents how proteins affect the expression levels of other proteins [2]. In the case when the network involves only a few genes and proteins, its dynamic properties can be studied directly in the laboratory by experimental techniques [3, 4]. However, if the network is formed of hundreds or thousands of different genes and proteins, then dissecting its dynamic behavior might be difficult and nonintuitive [5, 6]. For this purpose, several computational techniques have been developed recently that help us understand some of the basic properties of these gene regulatory networks (for an extensive review see [7, 8, 9]). Some of the most common modeling techniques involve the use of graphs [10, 11], Boolean networks [12, 13, 14], Bayesian networks [15], Petri nets [16, 17], reverse engineering methods [18], and coupled differential equations (linear [19], nonlinear [20, 21, 22], partial [23], stochastic [24, 25, 26], and delayed [27, 28, 29, 30, 31, 32, 33]).

Biologically, transcription and translation are the main processes by which a cell expresses the instructions encoded in its genes. **Transcription** is the first step in gene expression and it includes the replication of a gene into messenger RNA (mRNA). The second step is the **translation** process, where the information in the mRNA is translated into a protein. From these two processes, mRNA and protein concentrations arise naturally as the main intracellular regulatory agents for gene expression [1, 2].

There are several mechanisms that the cell uses to regulate levels of mRNA and protein concentrations. One important mechanism is the cell's ability to adjust and control the **degradation rates** of mRNA and proteins by increasing or decreasing the concentration of enzymes that degrade these. Another important example is the cell's ability to regulate the **transcription rate** of a specific gene. This is usually accomplished by a special type of proteins called *transcription factors*, which either promote or repress mRNA production by binding directly to the gene. In this work, we consider a network of transcription factors where the expression of a gene is regulated by several proteins. Figure 1 shows a basic mRNA-protein feedback mechanism which arises when the protein product returns to the nucleus as a transcription factor and slows down the transcription of its own mRNA by binding to the gene's promoter site [3, 34].

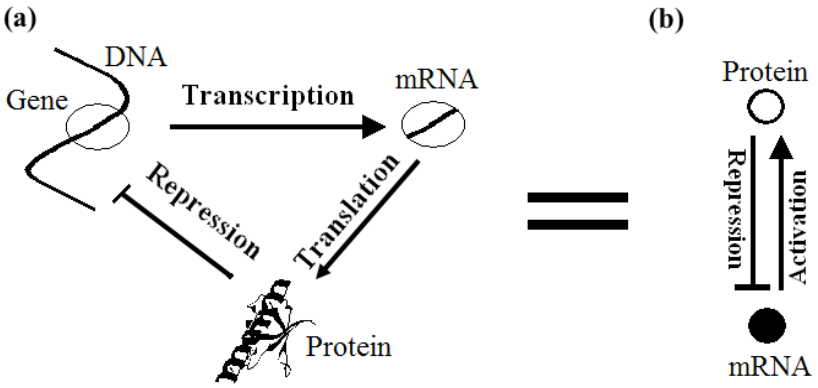

Figure 1: (a) Feedback inhibition mechanism. The gene is copied onto mRNA, which then attaches to a ribosome and a protein is produced. The protein then diffuses back into the nucleus where it represses the transcription of its own gene. (b) Compact notation for the mRNA-protein feedback loop for a single gene network system. Here the arrow ($\uparrow$) represents activation and the perpendicular symbol ($\perp$) represents repression.

Previous findings [34, 35] show that there are time delays associated with the feedback mechanism presented in Figure 1. These delays arise naturally as transcriptional delays (time it takes the gene to get copied into mRNA) and translational delays (time it takes the ribosome to translate mRNA into protein). Furthermore, recent studies [29, 34, 35] have shown that if we ignore translational delays (thus considering only transcriptional delays) we would still have an accurate dynamic model. As explained in [29] and [34], the ordinary differential equations (ODEs) associated to this system are given as follows:

$$\frac{dM}{dt} = -\mu_M\, M(t) + H\left(P(t-T)\right) \tag{1}$$

$$\frac{dP}{dt} = \alpha_P\, M(t) - \mu_P\, P(t) \tag{2}$$

where the time dependent variables are mRNA concentration, $M(t)$, its associated protein concentration, $P(t)$, the constants μ_M and μ_P are the degradation rates of the mRNA and protein, α_P is the rate of production of new protein molecules per mRNA molecule, and $H(P(t-T))$ is a Hill function representing the rate of *delayed* production of new mRNA molecules. We assume that $H(P(t-T))$ is a decreasing function of the concentration of protein present at a previous time $P(t-T)$, where T represents the transcriptional time delay.

The rest of the paper is organized as follows. Section 2 gives the main biological and geometrical background followed by the mathematical equations for both models: a *discrete* model characterized by a system of $N+1$ ODEs coupled to $N+1$ delay differential equations (DDEs); and a *continuous* model described by a partial differential equation (PDE) coupled to a delay differential-integral equation (DDIE). In Section 3 we present the associated linear stability analyses for both models and in Section 4 we characterize their steady state solutions. Linear analysis reveals the existence of a critical delay where steady states become unstable. Closed form expressions for the critical delay T_{cr} and associated frequency ω are then found. In Section 5 we confirm our results for the exponential weighting case by discretizing the continuous system into a $(2N+2)$-dimensional system and showing that the discrete critical delays approach the continuous T_{cr} as N becomes large. Finally, in Section 6 we discuss our findings.

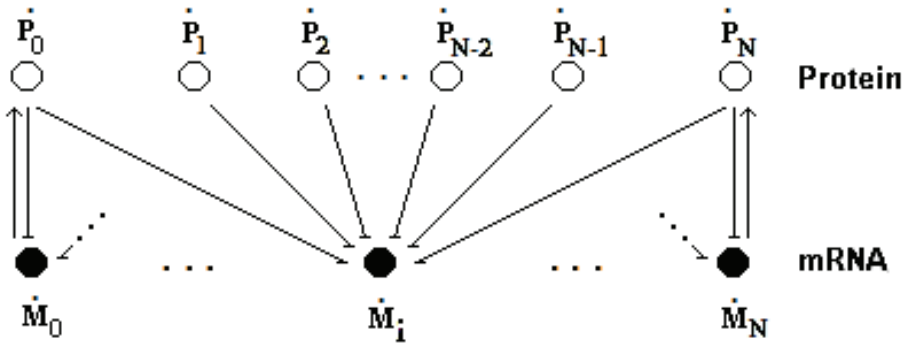

Figure 2: Geometric representation of the N+1 coupled system. The protein of the ith gene (p_i) represses its own mRNA production (m_i) and the mRNA production of all other N genes.

2 Mathematical Model

In this section we generalize the single gene model given by Equations (1) and (2). Figure 2 shows a network of N+1 genes where each mRNA, M_i, produces a protein, P_i. We assume that each of these transcription factor, P_i, regulates mRNA production by repressing all other M_j's in the network. The latter set up only affects the ODE associated to production of mRNA and thus translates the associated one-dimensional system given by Figure 1 into the following $(2N+2)$-dimensional system

$$\dot{M}_i = -\mu_M M_i + \alpha_M \sum_{j=0}^{N} H\left(P_j(t-T)\right) \tag{3}$$

$$\dot{P}_i = \alpha_P M_i - \mu_P P_i \tag{4}$$

where $i = 0, 1, \ldots, N$, and where we assume the same delay, T, and the same degradation rates for all mRNA-protein feedback loops.

We now transform the discrete model into a continuous model. We start by replacing the discrete concentrations of mRNA, M_i, and protein, P_i, by the concentration densities $M(x)$ and $P(x)$ respectively. This may be accomplished by tagging a given gene with a variable $x \in [0, 1]$ as depicted in Figure 3. The two are related by the following approximations

$$M_i = \int_{x_i}^{x_i+h} M(\bar{x})\, d\bar{x} \approx M(x_i)\, h \qquad \text{(small } h\text{)} \tag{5}$$

$$P_i = \int_{x_i}^{x_i+h} P(\bar{x})\, d\bar{x} \approx P(x_i)\, h \qquad \text{(small } h\text{)} \tag{6}$$

where we have omitted the time dependence notation for convenience and where we assume $x_0 = 0$ and $x_N = L$ (see Fig.2). Notice that Equations (5) and (6) yield

$$\sum_{j=0}^{N} H\left(P_j(t-T)\right) \approx \frac{1}{h} \sum_{j=0}^{N} H\left(P_j(t-T)\right) \approx \frac{1}{h} \int_0^L H\left(P_d(\bar{x})\right)\, d\bar{x} \tag{7}$$

where the second approximation is obtained by taking the limit as $h \to 0$ and where $P_d(\bar{x}) = P(\bar{x}, t-T)$. Next we divide (3)-(4) by h and use the approximations (5)-(7) to obtain the following continuous version

$$\dot{M}(x) = -\mu_m M(x) + \tilde{\alpha}_m \int_0^L H(p_d(\bar{x}))\, d\bar{x} \tag{8}$$

$$\dot{P}(x) = \alpha_p M(x) - \mu_p P(x) \tag{9}$$

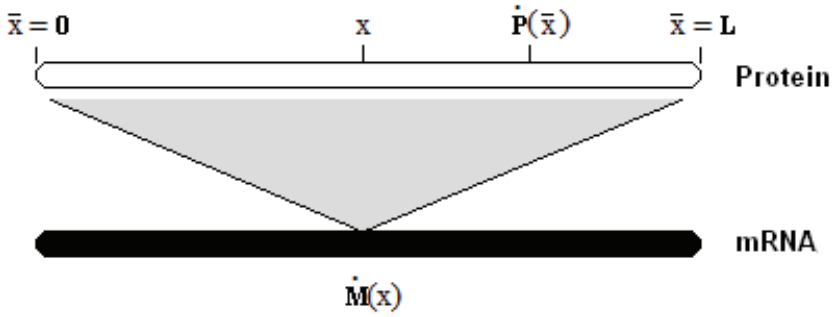

Figure 3: Geometric representation of the continuous model. We extend the discrete concentrations of mRNA, M_i, and protein, P_i, by the concentration densities $M(x)$ and $P(x)$ respectively. This may be accomplished by tagging a given gene with a variable $x \in [0,1]$ and thus extending the discretized geometry presented in Figure 2 to a continuum over both variables.

where $\tilde{\alpha}_m = \frac{\alpha_m}{h^2}$ and where its geometric representation is given by Figure 3.

In this study we will consider a rescaled version of Equations (8) and (9), which we obtain by using the following set of rescaled variables

$$m = \frac{M}{\tilde{\alpha}_m}, \quad p = \frac{P}{\tilde{\alpha}_m \alpha_p}, \quad p_0 = \frac{P_0}{\tilde{\alpha}_m \alpha_p} \tag{10}$$

thus yielding the following rescaled continuous system

$$\dot{m} = -\mu\, m + \int_0^1 K(x-\bar{x}) H(p_d(\bar{x}))\, d\bar{x} \tag{11}$$

$$\dot{p} = m - \mu\, p \tag{12}$$

where $m = m(x,t)$, $p = p(x,t)$, and $p_d(\bar{x}) = p(\bar{x}, t-T)$, and where we assume $\mu_p = \mu_m = \mu$ for simplicity. In addition, we have included a weighting function, $K(x-\bar{x})$, that generalizes system (8)-(9) by taking into account the "weight" or influence that a given gene has over other nearby genes. We consider two special cases of this weight function: uniform and exponential weighting. We explain both of these in the following subsections.

An important remark about the continuous model is that it is not a continuum over space, but rather the continuity is over the genes and their mRNA and protein products. Biologically, genes are discrete since they are organized separately along the DNA. Thus the discrete model is more realistic. Mathematically, on the other hand, we may approximate the discrete system by assuming a "gene continuum" between the genes and their mRNA and protein products. Thus, although we have sacrificed biological realism for mathematical tractability, we are now able to transform the multidimensional DDE system (3)-(4) into a more compact mathematical model of two coupled DDIEs given by (11) and (12). The latter approach is not an uncommon technique, since it has been used before on studies of predator-prey models [36], cancer resistance [37], epidemiology and population dynamics [38], all of which are inherently discrete biological systems but which have been conveniently extended to continuous models for their analysis.

2.1 Uniform Weighting

This case is characterized by the choice $K(x-\bar{x}) = 1$. Here each ribosome produces a given quantity of protein which is shared equally amongst all gene sites (see Fig. 4). For the rate of production of mRNA

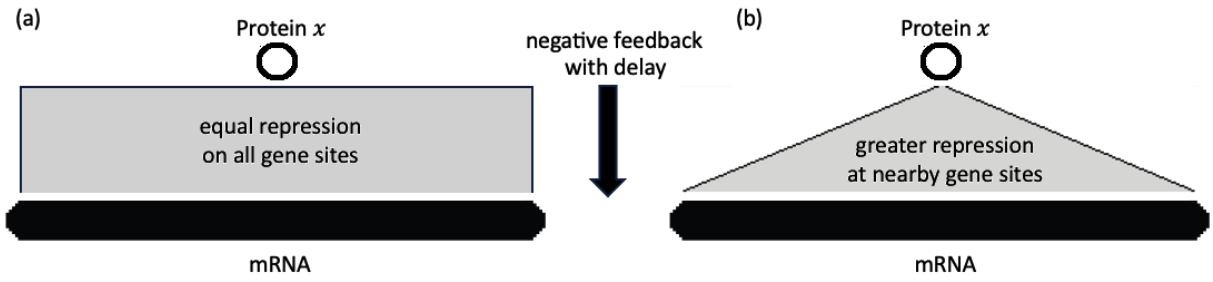

Figure 4: Feedback inhibition mechanism with different repression densities. (a) Uniform weighting where each protein represses equally all mRNA gene sites. (b) Exponential weighting where each protein represses nearby gene sites with a greater extent than more distant ones.

$H(p_d(\bar{x}))$ we choose the following Hill function [29, 34]:

$$H(p_d(\bar{x})) = \frac{1}{1+\left(\frac{p_d(\bar{x})}{p_0(\bar{x})}\right)^n} \tag{13}$$

where $p_d(\bar{x}) = p(\bar{x}, t-T)$ is the delayed protein concentration at location $\bar{x}$, and where $p_0(\bar{x})$ is a reference concentration of protein at $\bar{x}$, and n is a parameter [34]. The resulting system is of the form

$$\dot{m} = -\mu\, m + \int_0^1 \frac{1}{1+\left(\frac{p_d(\bar{x})}{p_0(\bar{x})}\right)^n}\, d\bar{x} \tag{14}$$

$$\dot{p} = m - \mu\, p \tag{15}$$

2.2 Exponential Weighting

This case is characterized by the choice $K(x-\bar{x}) = e^{-|x-\bar{x}|}$. Here each protein product is shared unequally, with nearby gene sites being repressed to a greater extent than more distant ones. For mathematical simplicity we choose the rate of production of mRNA $H(p_d(\bar{x}))$ to be given by a linear function of p_d:

$$H(p_d(\bar{x})) = 1 - p_d(\bar{x}) \tag{16}$$

The resulting system is of the form:

$$\dot{m} = -\mu\, m + \int_0^1 e^{-|x-\bar{x}|}(1-p_d(\bar{x}))\, d\bar{x} \tag{17}$$

$$\dot{p} = m - \mu\, p \tag{18}$$

3 Linear Stability Analysis

In this section we study the steady states of the system (11) and (12). Setting $\dot{p}$=$\dot{m}$=0 we see that at steady state m^*=μp^* and p_d^*=p^*, where a * represents the steady state solution.

3.1 Uniform Weighting

At steady state, Equations (14),(15) give

$$\mu^2 p^*(x) = \int_0^1 \frac{1}{1+\left(\frac{p^*(\bar{x})}{p_0(\bar{x})}\right)^n}\, d\bar{x} \tag{19}$$

Since the RHS of Equation (19) is independent of x, we see that $p^*(x)$=p^* is a constant. Because of the difficulty in evaluating the integral in Equation (19) for a general function $p_0(\bar{x})$, numerical integration is required in order to obtain an approximate value for p^*. In order to illustrate the process we choose a tractable function $p_0(\bar{x}) = 1 + \bar{x}$, together with $n = 3$ and $\mu = 0.2$, in which case Equation (19) gives $p^* = 2.9876$.

3.2 Exponential Weighting

At steady state, Equations (17),(18) give

$$\mu^2 p^*(x) \;=\; \int_0^1 e^{-|x-\bar{x}|} H(p^*(\bar{x}))\, d\bar{x} \tag{20}$$

which may be written in the form:

$$\mu^2 p^*(x) \;=\; e^{-x} \int_0^x e^{\bar{x}} H(p^*(\bar{x}))\, d\bar{x} \;+\; e^{x} \int_x^1 e^{-\bar{x}} H(p^*(\bar{x}))\, d\bar{x} \tag{21}$$

Differentiating Equation (21) twice [40] we obtain the equivalent second order ODE for the steady state solution p^*=$p^*(x)$:

$$\frac{d^2 p^*}{dx^2} - p^* \;=\; -\frac{2}{\mu^2} H(p^*) \tag{22}$$

where the boundary conditions are given by

$$p^*(0) \;=\; \frac{1}{\mu^2} \int_0^1 e^{-\bar{x}} H(p^*(\bar{x}))\, d\bar{x} \tag{23}$$

$$p^*(1) \;=\; \frac{1}{e\mu^2} \int_0^1 e^{\bar{x}} H(p^*(\bar{x}))\, d\bar{x}. \tag{24}$$

For the choice of $H(p(\bar{x}))$ given by (16), Equation (22) becomes

$$\frac{d^2 p^*}{dx^2} - \gamma\, p^* \;=\; 1 - \gamma \tag{25}$$

where

$$\gamma \;=\; 1 + \frac{2}{\mu^2} \;>\; 0 \tag{26}$$

Thus

$$p^*(x) \;=\; c_1 \sinh\sqrt{\gamma}\, x \;+\; c_2 \cosh\sqrt{\gamma}\, x \;+\; \frac{2}{\mu^2 \gamma} \tag{27}$$

where c_1 and c_2 are determined by substituting Equation (27) into (23) and (24):

$$c_1 \;=\; \left(1 - e^{\sqrt{\gamma}}\right) K \tag{28}$$

$$c_2 \;=\; \left(1 + e^{\sqrt{\gamma}}\right) K \tag{29}$$

where

$$K \;=\; \frac{1 - \sqrt{\gamma} - \left(1 + \sqrt{\gamma}\right)\, e^{\sqrt{\gamma}}}{\gamma \left[\left(\mu^2 \sqrt{\gamma} + \mu^2 + 1\right)\, e^{2\sqrt{\gamma}} + \mu^2 \sqrt{\gamma} - \mu^2 - 1\right]} \tag{30}$$

For example, in the case that $\mu = 0.2$, we obtain

$$p^*(x) \;=\; 0.12040 \sinh\sqrt{51}\, x \;-\; 0.12059 \cosh\sqrt{51}\, x \;+\; \frac{50}{51} \tag{31}$$

4 Stability of Steady States

To study the stability of the steady state solution $(m^*(x), p^*(x))$, we set $p(x,t) = p^*(x) + \eta(x,t)$ and $m(x,t) = m^*(x) + \xi(x,t)$ and linearize the resulting Equations in $\eta(x,t)$ and $\xi(x,t)$.

4.1 Uniform Weighting

Here the steady state solution p^* is constant in x. Equations (14),(15) give

$$\dot{\xi} = -\mu\xi - \int_0^1 K_1(\bar{x})\,\eta_d(\bar{x})\,d\bar{x} \tag{32}$$

$$\dot{\eta} = \xi - \mu\eta \tag{33}$$

where

$$K_1(\bar{x}) = \frac{n\beta}{(1+\beta)^2\,p^*}\,, \quad \text{where} \quad \beta = \beta(\bar{x}) = \left(\frac{p^*}{p_0(\bar{x})}\right)^n. \tag{34}$$

To study the stability of the origin we assume solutions of the form

$$\xi(x,t) = A(x)\,e^{\lambda t}\,, \qquad \eta(x,t) = B(x)\,e^{\lambda t} \tag{35}$$

and substitute them into Equations (32) and (33). Solving for $B(x)$ yields the following integral Equation

$$r\,B(x) = \int_0^1 K_1(\bar{x})\,B(\bar{x})\,d\bar{x} \tag{36}$$

where

$$r = -e^{\lambda T}(\lambda+\mu)^2 \tag{37}$$

To solve Equation (36), we note that the RHS is independent of x, which tells us that $B(x)$=B is constant. Eliminating B from Equation (36), we obtain

$$r = \int_0^1 K_1(\bar{x})\,d\bar{x} \tag{38}$$

Here $K_1(\bar{x})$ is given by Equation (34), so that r is known. We are left with the problem of determining λ from Equation (37) when r is known. This problem is common to both the present case of uniform weighting as well as to the case of exponential weighting. To avoid repeating the treatment, we handle this problem in the Appendix. There are two important situations: (i) when $T = 0$, in which case λ determines the stability of the system with no delay, and (ii) when $T = T_{cr}$, where the delay T_{cr} corresponds to pure imaginary λ and corresponds to a change in stability.

(i) When $T = 0$, Equation (64) in the Appendix gives

$$\lambda = -\mu \pm \sqrt{-\int_0^1 K_1(\bar{x})\,d\bar{x}} \tag{39}$$

which shows that the system with no delay is stable since $K_1(\bar{x})$>0 from (34).

(ii) When $T = T_{cr}$, Equations (69),(68) in the Appendix give

$$T_{cr} = \frac{1}{\omega}\arctan\left(\frac{2\omega\mu}{\omega^2-\mu^2}\right) \tag{40}$$

$$\omega = \sqrt{-\mu^2 + \int_0^1 K_1(\bar{x})\,d\bar{x}} \tag{41}$$

We continue the example given in the previous section, namely, $p_0(\bar{x}) = 1 + \bar{x}$, $n = 3$ and $\mu = 0.2$, which yielded the steady state $p^* = 2.9876$. By substituting Equation (34) into (41) we obtain $\omega = 0.24977$ which we substitute into (40) to obtain the critical delay $T_{cr} = 5.40638$, where the steady state becomes unstable.

4.2 Exponential Weighting

In this case the steady state $p^*(x)$ satisfies the ODE (22). To study its stability, we linearize Equations (17) and (18), which give

$$\xi_t = -\mu\,\xi - \int_0^1 e^{-|x-\bar{x}|}\,\eta_d(\bar{x})\,d\bar{x} \tag{42}$$

$$\eta_t = \xi - \mu\,\eta \tag{43}$$

If $\xi(x,t)=\phi(x)e^{\lambda t}$ and $\eta(x,t)=\psi(x)e^{\lambda t}$ then Equations (42) and (43) become

$$-e^{\lambda T}\,(\lambda+\mu)\phi(x) = \int_0^1 e^{-|x-\bar{x}|}\,\psi(\bar{x})\,d\bar{x} \tag{44}$$

$$(\lambda+\mu)\psi(x) = \phi(x) \tag{45}$$

Substituting Equation (45) into (44) gives

$$r\,\psi(x) = \int_0^1 e^{-|x-\bar{x}|}\,\psi(\bar{x})\,d\bar{x} \tag{46}$$

where r is given by Equation (61). Next we transform the integral Equation (46) to the following equivalent second order ODE [40]

$$\frac{d^2\psi}{dx^2} + \left(\frac{2}{r} - 1\right)\,\psi = 0 \tag{47}$$

which will have solutions of the form

$$\psi(x) = c_1\,\sin(\rho\,x) + c_2\,\cos(\rho\,x) \tag{48}$$

where c_1 and c_2 are constants and $\rho = \sqrt{\frac{2}{r} - 1}$. The endpoint boundary conditions of the second order ODE (47) are obtained from Equation (46) as follows

$$\psi(0) = \frac{\rho^2+1}{2}\int_0^1 e^{-\bar{x}}\psi(\bar{x})\,d\bar{x} \tag{49}$$

$$\psi(1) = \frac{\rho^2+1}{2e}\int_0^1 e^{\bar{x}}\psi(\bar{x})\,d\bar{x}. \tag{50}$$

Substituting Equation (48) into (49) and (50) gives a system of Equations on the constants c_1 and c_2 which yields the following condition on ρ for nontrivial solutions

$$\begin{vmatrix} \rho\,\sin\rho - \cos\rho - e & -\sin\rho - \rho\,\cos\rho + e\,\rho \\ e\,\rho\,\sin\rho - e\,\cos\rho - 1 & -e\,\sin\rho - e\,\rho\,\cos\rho + \rho \end{vmatrix} = 0 \tag{51}$$

or equivalently

$$\left(\rho^2 - 1\right)\,\sin\rho - 2\,\rho\,\cos\rho = 0. \tag{52}$$

Equation (52) has an infinite number of roots, the first three of which are $\rho = 1.30654$, 3.67319, 6.58462, ... which give the following corresponding values for $r = 2/(1+\rho^2) = 0.73881$, 0.13800, 0.04509, ... Now that we know r, we may use the results in the Appendix to determine stability of the steady state.

(i) When $T = 0$, Equation (64) in the Appendix gives $\lambda = -\mu \pm \sqrt{-r}$ which, in view of the fact that all the values of r are positive, shows that the system with no delay is stable.

(ii) When $T = T_{cr}$, Equations (68) and (69) in the Appendix give expressions for ω and T_{cr}. Since we are interested in the smallest value for T_{cr}, we take $r = 0.73881$, which gives, for $\mu = 0.2$, the values $\omega = 0.83595$ and $T_{cr} = 0.56184$.

5 Numerical Analysis

To check our previous results, we replace the continuous variables $\xi(x,t)$ and $\eta(x,t)$ in Equations (42),(43) by a discrete set of $N+1$ variables $\xi_i(t)$ and $\eta_i(t)$. This corresponds to a model of $N+1$ coupled gene units, and replaces the integral in Equation (42) by a sum of $N+1$ terms. As we now demonstrate, analysis of this system shows that $T_{cr} \to 0.56184$ as N goes to infinity, for $\mu = 0.2$, in agreement with the foregoing analysis. We start by discretizing the continuous system, Equations (42),(43), into an $(2N+2)$-dimensional system given by

$$\dot{\xi}_i = -\mu\,\xi_i - \frac{1}{N+1}\sum_{j=0}^{N} e^{-|i-j|/N}\,\eta_j(t-T) \tag{53}$$

$$\dot{\eta}_i = \xi_i - \mu\,\eta_i \tag{54}$$

where $i = 0, 1, \ldots, N$. Next we assume solutions of the form

$$\xi_i = \phi_i\, e^{\lambda t} \tag{55}$$

$$\eta_i = \psi_i\, e^{\lambda t} \tag{56}$$

and substitute them into (53),(54) to obtain

$$-e^{\lambda T}(\lambda+\mu)\,\phi_i = \frac{1}{N+1}\sum_{j=0}^{N} e^{-|i-j|/N}\,\psi_j \tag{57}$$

$$(\lambda+\mu)\,\psi_i = \phi_i \tag{58}$$

eliminating ϕ_i we obtain

$$c\,\psi_i = \sum_{j=0}^{N} e^{-|i-j|/N}\,\psi_j \tag{59}$$

where $c = (N+1)r$ and r is given by (61). For nontrivial solutions, the system (59) of $N+1$ algebraic Equations, must satisfy $\det(K - cI) = 0$ where K is the $(N+1)\times(N+1)$ matrix $K=[K_{ij}]=[\exp(-|i-j|/N)]$ and c is its associated eigenvalue. Since K is a symmetric matrix, all of its eigenvalues are real and thus c is a real number. Numerical evaluation of these eigenvalues c shows that they are all positive. The stability results for the steady state are summarized as follows:

(i) When $T = 0$, we see from Equation (64) in the Appendix with $r = c/(N+1)$ that the steady state in the system with no delay is stable.

(ii) When $T = T_{cr}$, we choose the smallest value of c for a given truncation size N, and use Equations (68) and (69) in the Appendix to obtain values for ω and T_{cr} where we take $r = c/(N+1)$. Table 1 shows results for $\mu = 0.2$ for various values of N.

Table 1: Numerical Results for $\mu = 0.2$

N	c	ω	T_{cr}
1	1.3678	0.8024	0.6089
2	2.0612	0.8044	0.6059
3	2.7844	0.8100	0.5977
5	4.2494	0.8175	0.5870
7	5.7215	0.8216	0.5813
10	7.9338	0.8253	0.5761
15	11.6246	0.8285	0.5718
30	22.7034	0.8320	0.5671
50	37.4783	0.8336	0.5649
100	74.4173	0.8348	0.5634
200	148.2960	0.8353	0.5627
300	222.1740	0.8355	0.5623

6 Conclusions

In this paper we investigated the steady state solutions of a continuous gene regulatory network model. The model takes the form of an ordinary differential equation coupled to a delay differential-integral equation having time, t, and gene location, x, as independent variables. The study was divided into two cases: uniform weighting and exponential weighting. For the uniform weighting case we showed that the steady state is not only constant in time but in space as well. This allowed us to solve the associated eigenvalue problem and prove that the system is stable when there is no delay. Subsequently, we showed that the system becomes unstable for a critical delay and found closed form expressions for the critical delay and associated frequency. For the exponential weighting case, we found that the steady state solution depends on gene location. This was accomplished by transforming the steady state integral equation into a second order differential equation. By solving the differential equation we found a closed form expression for the x-dependent steady state. Stability analysis then revealed that the nondelayed system is stable and expressions for the critical delay and associated frequency were found.

We confirmed our results by means of a numerical approximation where the continuous system was discretized, which resulted in a $(2N+2)$-dimensional system with delay. Numerical evaluations for different N were performed and good agreement was found with the continuous counterpart as N became large. This work thus provides an algorithm to construct a system of two equations (an ODE coupled to a DDIE) which preserves the same dynamic features as a multidimensional ODE system of a large gene network. In particular, we have shown that a Hopf bifurcation is conserved in both systems by calculating the critical values of the delay and showing that $T_{cr}^{discrete} \to T_{cr}^{continuous}$. It is hoped that our approach will be useful to researchers in the field of gene networks, by helping avoid cumbersome numerical routines for large systems of ODEs.

7 Appendix

In Equations (36) and (46) we have the following eigenvalue problem

$$r\, f(x) \;=\; \int_0^1 K(x,\bar{x}) f(\bar{x}) d\bar{x} \tag{60}$$

where $K(x,\bar{x})$ is a *symmetric* integral kernel, $f(x)$ is the eigenfunction, and r is the associated eigenvalue given by

$$r \;=\; -\, e^{\lambda T}(\lambda+\mu)^2 \tag{61}$$

Note that r is real since the RHS of (60) contains a symmetric kernel and thus is a self-adjoint operator of the form

$$L(\cdot) = \int_0^1 K(x, \bar{x})(\cdot)\, d\bar{x} \tag{62}$$

which has real eigenvalues.

Now given r we wish to determine λ in two special situations: (i) when $T = 0$, and (ii) when $T = T_{cr}$ and λ is pure imaginary, corresponding to a change in stability.

(i) When $T = 0$, Equation (61) becomes

$$r = -(\lambda + \mu)^2 \tag{63}$$

and gives

$$\lambda = -\mu \pm \sqrt{-r} \tag{64}$$

If $r > 0$ then the $\mathrm{Re}(\lambda) = -\mu < 0$ (for positive μ), and we have stability of the system with no delay.

(ii) When $T = T_{cr}$ and $\lambda = i\omega$, Equation (61) becomes

$$r = -e^{i\omega T_{cr}}(i\omega + \mu)^2 \tag{65}$$

which gives the two real equations

$$r = 2\,\mu\,\omega\, \sin(\omega T_{cr}) + \left(\omega^2 - \mu^2\right) \cos(\omega T_{cr}) \tag{66}$$

$$0 = \left(\omega^2 - \mu^2\right) \sin(\omega T_{cr}) - 2\,\mu\,\omega\, \cos(\omega T_{cr}) \tag{67}$$

Solving Equations (66) and (67) for $\sin(\omega T_{cr})$ and $\cos(\omega T_{cr})$, and using the identity $\sin^2(\omega T_{cr}) + \cos^2(\omega T_{cr}) = 1$ we obtain

$$\omega = \sqrt{r - \mu^2} \tag{68}$$

Dividing the expressions for $\sin \omega T_{cr}$ and $\cos \omega T_{cr}$ and solving for T_{cr} we also obtain

$$T_{cr} = \frac{1}{\omega} \arctan\left(\frac{2\mu\omega}{\omega^2 - \mu^2}\right) \tag{69}$$

References

[1] Alberts B., Johnson, A., Lewis, J., Morgan D., Raff M., Roberts K., Walter P. (2015) *Molecular Biology of the Cell.* Garland Science.

[2] Ay A., Arnosti D. N. (2011) Mathematical modeling of gene expression: a guide for the perplexed biologist. *Crit. Rev. Biochem. Mol. Biol.,* **46(2)**, 137–151.

[3] Elowitz M.B., Leibler S. (2000) A synthetic oscillatory network of transcriptional regulators. *Nature,* **403**, 335–338.

[4] Gardner T.S., Cantor C.R., Collins J.J. (2000) Construction of a genetic toggle switch in Escherichia coli. *Nature,* **403**, 339–342.

[5] Ciliberti A., Novak B., Tyson J.J. (2005) Steady states and oscillations in the p53/Mdm2 network. *Cell Cycle,* **4(3)**, 488–493.

[6] Muller S., Hofbauer J., Endler L., Flamm C., Widder S., Schuster P. (2006) A generalized model of the repressilator. *J. Math. Biol.,* **53**, 905–937.

[7] Hasty J., McMillen D., Isaacs F., Collins J.J. (2001) Computational studies of gene regulatory networks: In numero molecular biology. *Nature,* **2**, 268–279.

[8] Jong H. (2002) Modeling and simulation of genetic regulatory systems: A literature review. *J. Comp. Biol.,* **9(1)**, 67–103.

[9] Schlitt T., Brazma A. (2007) Current approaches to gene regulatory network modelling. *BMC Bioinformatics,* **8**, S9.

[10] Kohn M.C., Lemieux D.R. (1991) Identification of regulatory properties of metabolic networks by graph theoretical modeling. *J. Theor. Biol.,* **150**, 3–25.

[11] Mincheva M., Roussel M.R. (2007) Graph-theoretic methods for the analysis of chemical and biochemical networks. II. Oscillations in networks with delays. *J. Math. Biol.,* **55**, 87–104.

[12] Chaves M., Albert R., Sontag E.D. (2005) Robustness and fragility of Boolean models for genetic regulatory networks. *J. Theor. Biol.,* **235**, 431–449.

[13] Oktem H., Pearson R., Egiazarian K. (2003) An adjustable aperiodic model class of genomic interactions using continuous time Boolean networks (Boolean delay equations). *Chaos,* **13(4)**, 1167–1174.

[14] Perkins T.J., Hallett M., Glass L. (2006) Dynamical properties of model gene networks and implications for the inverse problem. *BioSystems,* **84**, 115–123.

[15] Friedman N., Linial M., Nachman I., Peer D. (2000) Using Bayesian networks to analyze expression data. *J. Comp. Biol.,* **7**, 601–620.

[16] Gambin A., Lasota S., Rutkowski M. (2006) Analyzing stationary states of gene regulatory network using Petri nets. *In Silico Biology,* **6**, 93–109.

[17] Matsuno H., Doi A., Nagasaki M., Miyano S. (2000) Hybrid Petri net representation of gene regulatory network. *Pac. Symp. Biocomput.,* **5**, 338–349.

[18] Tegner J., Yeung M.K.S., Hasty J., Collins J.J. (2003) Reverse engineering gene networks: Integrating genetic perturbations with dynamical modeling. *PNAS,* **100(10)**, 5944–5949.

[19] Jong H., Gouze J., Hernandez C., Page M., Sari T., Geiselmann J. (2004) Qualitative simulation of genetic regulatory networks using piecewise-linear models. *Bulletin of Mathematical Biology,* **66**, 301–340.

[20] Conrad E.D., Tyson J.J. (2006) *Modeling molecular interaction networks with nonlinear ordinary differential equations.* Cambridge, MA: MIT Press, 97–123.

[21] Hasty J., Dolnik M., Rottschafer V., Collins J.J. (2002) Synthetic gene network for entraining and amplifying cellular oscillations. *Phys. Rev. Let.,* **88(14)**, 148101.

[22] Mochizuki A. (2007) Structure of regulatory networks and diversity of gene expression patterns. *J. Theor. Biol.,* **250(2)**, 307–321.

[23] Turner S., Sherratt J.A., Painter K.J. (2004) From a discrete to a continuous model of biological cell movement. *Phys. Rev. E,* **69**, 021910.

[24] Goutsias J., Kim S. (2006) Stochastic transcriptional regulatory systems with time delays: A mean-field approximation. *J. Comp. Biol.,* **13(05)**, 1049–1076.

[25] Ribeiro A., Zhu R., Kauffman S.A. (2006) A general modeling strategy for gene regulatory networks with stochastic dynamics. *J. Comp. Biol.,* **13(9)**, 1630–1639.

[26] Zhu R., Ribeiro A.S., Salahub D., Kauffman S.A. (2007) Studying genetic regulatory networks at the molecular level: Delayed reaction stochastic models. *J. Theor. Biol.,* **246**, 725–745.

[27] Bratsun D., Volfson D., Tsimring L.S., Hasty J. (2005) Delay-induced stochastic oscillations in gene regulation. *PNAS,* **102(41)**:14593–14598.

[28] Edwards R., van den Driessche P., Wang L. (2007) Periodicity in piecewise-linear switching networks with delay. *J. Math. Biol.,* **55**, 271–298.

[29] Verdugo A., Rand R. (2008) Hopf bifurcation in a DDE model of gene expression. *Communications in Nonlinear Science and Numerical Simulation,* **13**, 235–242.

[30] Verdugo A., Rand R. (2008) DDE Model of Gene Expression: A Continuum Approach. *Proceedings of DSCC, ASME 2008 Dynamic Systems and Control Conference,* **DSCC2008-160**, 1–7.

[31] Khajanchi S., Nieto J. (2019) Mathematical modeling of tumor-immune competitive system, considering the role of time delay. *Applied Mathematics and Computation,* **340**, 180–205.

[32] Zhang Z., Yin X., Gao Z. (2022) Non-flocking and flocking for the Cucker-Smale model with distributed time delays. *Journal of the Franklin Institute,* **In Press**, https://doi.org/10.1016/j.jfranklin.2022.03.028.

[33] Zhou Y., Gao Y. (2022) Fixed-Time Synchronization Analysis of Genetic Regulatory Network Model with Time-Delay. *Symmetry,* **14**, 951.

[34] Monk N.A.M. (2003) Oscillatory expression of Hes1, p53, and NF-κB driven by transcriptional time delays. *Current Biology,* **13**, 1409–1413.

[35] Lewis J. (2003) Autoinhibition with transcriptional delay: A simple mechanism for the zebrafish somitogenesis oscillator. *Current Biology,* **13**, 1398–1408.

[36] Leard B., Rebaza J. (2011) Analysis of predator?prey models with continuous threshold harvesting. *Applied Mathematics and Computation,* **217(12)**, 5265–5278.

[37] Greene J., Lavi O., Gottesman M., Levy D. (2014) The Impact of Cell Density and Mutations in a Model of Multidrug Resistance in Solid Tumors. *Bull. Math. Biol.,* **76(3)**, 627–653.

[38] Brauer F., Castillo-Chavez C. (2012) Continuous Population Models. *Mathematical Models in Population Biology and Epidemiology,* **Springer**, 3–47.

[39] Casey R., Jong H., Gouze J. (2006) Piecewise-linear models of genetic regulatory networks: Equilibria and their stability. *J. Math. Biol.,* **52**, 27–56.

[40] Hildebrand F.B. (1965) *Methods of Applied Mathematics.* Prentice Hall.

[41] Mestl T., Plahte E., Omholt S.W. (1995) A mathematical framework for describing and analysing gene regulatory networks. *J. Theor. Biol.,* **176**, 291–300.

[42] Smith J., Theodoris C., Davidson E.H. (2007) A gene regulatory network subcircuit drives a dynamic pattern of gene expression. *Science,* **318**, 794–797.

[43] Tyson J.J., Chen K.C., Novak B. (2001) Network dynamics and cell physiology. *Nature Rev,* **2(12)**, 908–916.

[44] Verdugo A., Rand R. (2008) Center manifold analysis of a DDE model of gene expression. *Communications in Nonlinear Science and Numerical Simulation,* **13**, 1112–1120.

[45] Zeiser S., Muller J., Liebscher V. (2007) Modeling the Hes1 Oscillator. *J. Comp. Biol.,* **14(7)**, 984–1000.